



1
2
3
4
5
6
7
8
9
10
11

Measurement Report: Urban Ammonia and Amines in Houston, Texas

Lee Tiszenkel¹, James Flynn², Shan-Hu Lee^{1*}

¹ Department of Atmospheric and Earth Sciences, University of Alabama at Huntsville;
Huntsville, Alabama, USA

² Department of Earth and Atmospheric Sciences, University of Houston; Houston, Texas,
USA

Corresponding author (shanhu.lee@uah.edu)



12 **Abstract.** Ammonia and amines play critical roles in secondary aerosol formation, especially in
13 urban environments. However, fast measurements of ammonia and amines in the atmosphere are
14 very scarce. We measured ammonia and amines with a chemical ionization mass spectrometer
15 (CIMS) at the urban center in Houston, Texas, the fourth most populated urban site in the United
16 States, during October 2022. Ammonia concentrations were on average 4 parts per billion in
17 volume (ppbv), while the concentration of an individual amine ranged from several parts per
18 trillion in volume (pptv) to hundreds of pptv. These reduced nitrogen compounds were more
19 abundant during the weekdays than on weekends and correlated with measured CO concentrations,
20 implying they were mostly emitted from pollutant sources. Both ammonia and amines showed a
21 distinct diurnal cycle, with higher concentrations in the warmer afternoon, indicating dominant
22 gas-to-particle conversion processes taking place with the changing ambient temperatures. Studies
23 have shown that dimethylamine is critical for urban new particle formation (NPF), but currently,
24 there are no amine emission inventories in global climate models (as opposed to ammonia). Our
25 observations show that amines in general positively correlated with ammonia, indicating that it is
26 reasonable for global models to use scaled-down ammonia concentrations (e.g., 0.1 %) as a proxy
27 of urban dimethylamine concentrations to simulate urban NPF processes.

28 1. Introduction

29

30 Atmospheric ammonia and amines are ubiquitous in the atmosphere, and they have been found
31 in the gas phase, aerosol, clouds, and fog droplets [*Ge et al.*, 2011a; b]. Ammonia and amines are
32 emitted from various natural and anthropogenic sources, such as agricultural activity, animal
33 husbandry, vegetation, soil, waste processing, automobile traffic, power plants, and biomass
34 burning [*Ge et al.*, 2011a]. Ammonia and amines often share the same emission sources. In general,
35 ambient concentrations of ammonia are at the parts per billion in volume (ppbv) range, and amines
36 are approximately two to three orders of magnitude lower than ammonia concentrations. Ambient
37 concentrations of ammonia and amines vary rapidly due to emission, gas-to-particle conversion,
38 and wet deposition processes [*You et al.*, 2014; *Yu and Lee*, 2012].

39 Laboratory studies have shown that ammonia and amines play key roles in new particle
40 formation (NPF) as they can stabilize sulfuric acid clusters [*Almeida et al.*, 2013; *Glasoe et al.*,
41 2015; *Jen et al.*, 2016; *Lehtipalo et al.*, 2018; *M Xiao et al.*, 2021; *Yu et al.*, 2012]. In particular,
42 dimethylamine can have a profound effect on atmospheric processes even at the pptv level
43 [*Almeida et al.*, 2013; *Glasoe et al.*, 2015]. Field observations show that ammonia and amines are
44 associated with NPF events in Chinese megacities [*R. Cai et al.*, 2021; *Runlong Cai et al.*, 2023;
45 *Yan et al.*, 2021; *Yao et al.*, 2016], urban areas in the United States [*Jen et al.*, 2016; *Smith et al.*,
46 2010], European cities [*J. Brean et al.*, 2020], a high altitude site [*Bianchi et al.*, 2016], and the
47 Arctic and Antarctic [*Beck et al.*, 2021; *James Brean et al.*, 2021; *Jokinen et al.*; *Köllner et al.*,
48 2017]. However, global models cannot simulate urban NPF processes currently because of the lack
49 of amine emission inventories in models.



50 Ammonia and amines also contribute to secondary organic aerosol (SOA) formation by
51 condensation of oxidation products formed by reactions with ozone, OH, or NO₃ radicals and
52 produce light-absorbing particles [Mark E. Erupe et al., 2010; Malloy et al., 2009; C. J. Nielsen,
53 2016; Claus J. Nielsen et al., 2012; Qiu and Zhang, 2013; Silva et al., 2008]. As a result, reducing
54 ammonia emissions has been identified as a cost-effective way to mitigate ambient fine particle
55 concentrations [Gu et al., 2021].

56 Fast-response measurements of ammonia and amines at atmospheric concentrations are very
57 challenging [Lee, 2022], although such measurements are necessary because these reduced
58 nitrogen compounds have relatively short atmospheric lifetimes [Claus J. Nielsen et al., 2012].
59 Previously, [Schwab et al., 2007] made an intercomparison of six different ammonia detection
60 methods in the laboratory and found a large variance in the measured concentrations and vastly
61 different response times (over several hours) within different instruments. Difficulties in the
62 detection of base compounds also arise because these “sticky” compounds can rapidly adsorb and
63 desorb on/from the surfaces of sampling inlets to cause background signals that vary depending
64 on ambient concentrations, air humidity, and other atmospheric conditions. Thus frequent, in situ
65 measurements of instrument background signals using proper zero gases are required, especially
66 for field observations with rapidly changing ambient concentrations of base compounds.

67 Chemical ionization mass spectrometers (CIMS) using ion reagents such as protonated ethanol,
68 acetone, and water ions can detect ammonia and amines in the atmosphere with fast response
69 [Benson et al., 2010; Hanson et al., 2011; Jen et al., 2016; Nowak et al., 2006; Yu and Lee, 2012
70]. As summarized in Table 1, CIMS technique has been used for the detection of ambient ammonia
71 and amines at a polluted site in Ohio [You et al., 2014; Yu and Lee, 2012], a rural Alabama forest
72 [You et al., 2014], and polluted urban sites in China [G Wang et al., 2016; M Wang et al., 2020a;
73 Zheng et al., 2015; Zhu et al., 2022]. As shown in Table 1, there are even fewer studies that
74 simultaneously measured ammonia and amines. The CIMS using ethanol reagent can measure
75 amines at or below single-digit pptv concentrations with a time response of 1 minute and measure
76 simultaneously amines and ammonia [Benson et al., 2010; M. E. Erupe et al., 2011; You et al.,
77 2014; Yu and Lee, 2012]. The CIMS using protonated water ions (i.e., proton-transfer chemical
78 ionization mass spectrometer, PTR-CIMS) can measure mono- and di-amines [Hanson et al.,
79 2011; Jen et al., 2016]. Using a high-resolution time-of-flight (HR-TOF) detector coupled to CIMS
80 (HR-TOF CIMS) (with ethanol reagent), [Yao et al., 2016] measured various amines and amides
81 in Shanghai. However, isomers of amines were still not resolved in the detection; for example, the
82 measured C₂-amines still contained dimethylamine and ethylamine. Thus, a major disadvantage
83 of a mass spectrometer (regardless of mass resolution) is the inability to resolve/identify isomers.
84 To resolve isomers, tandem MS/MS analysis or an additional independent separation method (such
85 as chromatography) coupled to the mass spectrometer is necessary.

86 In situ measurements of ammonia have been made in various atmospheric environments also
87 with optical techniques such as open-path absorption [Miller et al., 2014], closed-path absorption
88 [Ellis et al., 2010; Griffith and Galle, 2000; Leen et al., 2013; McManus et al., 2010; Pollack et
89 al., 2019], cavity ring-down spectroscopy [Martin et al., 2016], and photoacoustic spectroscopy



90 [Pushkarsky *et al.*, 2002]. These fast-response optical techniques were used for flux and aircraft
91 measurements of ammonia.

92 We measured ammonia and C1-C6 amines with an ethanol CIMS in October 2022 at the urban
93 center in Houston, Texas. Houston is the fourth most populated urban center in the U.S. and
94 contains a diverse range of pollutant emissions from urban activity, traffic, ship channels, oil
95 production, marine air masses, and agricultural activity. The primary goal of these measurements
96 is to quantify ammonia and C1-C6 amines in an urban setting and identify the atmospheric
97 conditions that affect their abundance. The study is amongst very few observations of ammonia
98 and amines at highly polluted urban sites in the U.S. We also compare observations in Houston
99 with previous measurements taken with the same instrument in Kent, Ohio (less polluted) [You *et*
100 *al.*, 2014] and establish a quantitative relationship between ammonia and dimethylamine in a
101 different range of polluted conditions. This relationship will allow global models to simulate urban
102 NPF processes using the existing ammonia emission inventories.

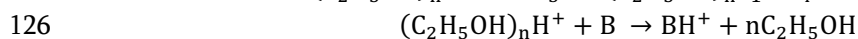
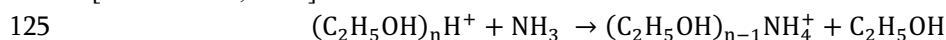
103

104 2. Methods

105

106 The field observation took place in Houston continuously from the 8th to the 27th of October in
107 2022. Measurements were made at a stationary platform located on the campus of the University
108 of Houston (29.72° N, 95.34° W) ~2.5 km from central downtown Houston. Maps of the
109 measurement site (Figs. 1 and S1). The measurement platform was located ~5 m from an active
110 parking lot, ~200 m from a low-traffic road, ~300 m from a high-traffic thoroughfare, and ~500 m
111 from an interstate highway. The immediate vicinity of the site was the University of Houston
112 campus, containing classroom buildings, dormitories, facilities services, and dining halls. Nearby
113 to the southeast of the site were several restaurants as well as an industrial park containing sites of
114 chemical supply companies, construction, machining services, and automobile shops. The site was
115 surrounded by residential areas to the south, northeast, and west. The city center and highest
116 population densities were to the northeast of the measurement site.

117 The ethanol CIMS instrument used has been described in detail previously [Benson *et al.*,
118 2010; Mark E. Erupe *et al.*, 2010; M. E. Erupe *et al.*, 2011; Lee Tiszenkel and Lee, 2023; L.
119 Tiszenkel *et al.*, 2019; You *et al.*, 2014; Yu and Lee, 2012]. The CIMS draws 10 standard liter per
120 minute (slpm) of sample air into a low-pressure ion-molecule region (about 2,000 Pa) where the
121 flow mixes with a pure nitrogen flow with a 2 slpm through a stainless-steel vessel of 200-proof
122 ethanol, followed by a ²¹⁰Po radiation source. Ammonia and amines were detected with the
123 following ion-molecule reactions based on [M. E. Erupe *et al.*, 2011], [Yu and Lee, 2012], and
124 [Nowak *et al.*, 2006]:

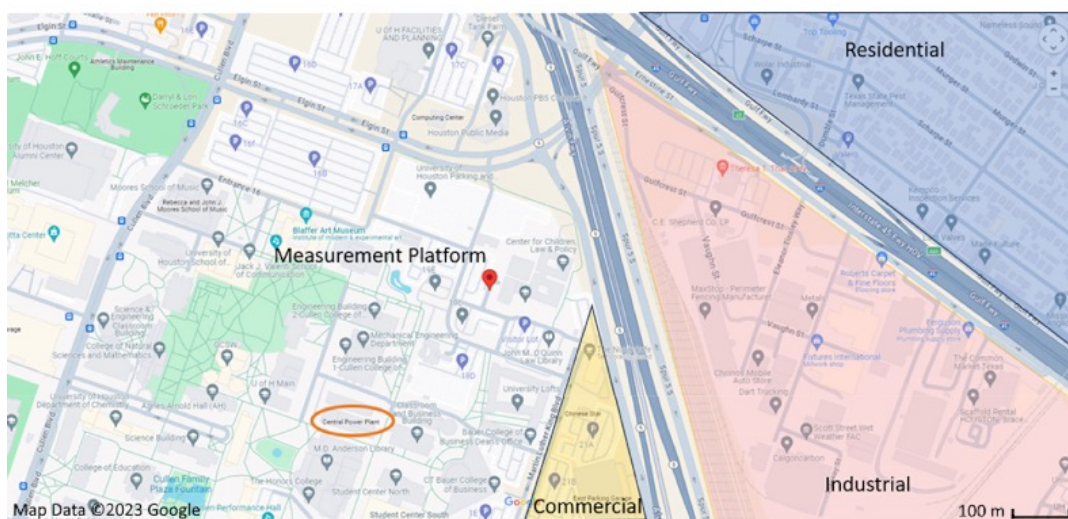


127 Here, “B” refers to amines, and “n” is the number of reagent ions measured by the CIMS (n=1-3).

128 The (C₂H₅OH)₂H⁺ (m/z = 93) peak was the highest among the three reagent ions (m/z = 47, 93,
129 and 140). As shown in Fig. S2, the production ions of amines were protonated ions: C1-amine (m/z



130 = 32), C2 ($m/z = 46$), C3 ($m/z = 60$), C4 ($m/z = 74$), C5 ($m/z = 88$), and C6 ($m/z = 102$). Ammonia
131 product ions were NH_4^+ ($m/z = 18$, higher peak) and $(\text{C}_2\text{H}_5\text{OH})\text{NH}_4^+$ ($m/z = 64$, lower peak); these
132 two ions were strongly correlated to each other during the ammonia calibration and ambient
133 measurements, indicating they represent ammonia signals.



134
135 **Fig. 1.** Location of the measurement platform, indicated by a red pin in the center of the map.
136 Nearby commercial, industrial, and residential areas are labeled by yellow, red, and blue shaded
137 sections, respectively. The nearby University of Houston power plant is circled in orange to the
138 southwest of the measurement platform. The map of the greater Houston urban area, as well as
139 the satellite view of the nearby vicinity of the measurement site, are shown in Fig. S1. Map
140 credit: © Google.

141
142

143 To obtain a background signal, the CIMS is operated with 10 minutes of sampling followed
144 by 10 minutes of background measurements. Figure S2 shows the main reagent and base
145 compound product ions during the switching between ambient and background measurements.
146 Background measurements were taken by switching a 3-way valve to supply the inlet with a flow
147 of zero air through a silicon phosphate medium (Pan Tech, Texas) to scrub ammonia and amines.
148 The reagent signal was taken as the sum of three ethanol reagent ions. Reagent ion signals were



149 typically around 400 kHz with less than 10 % difference between ambient and background
150 measurement modes. Ammonia and amine concentrations were calculated by the difference
151 between the ambient and background signals normalized to 1,000,000 Hz of reagent ion signal
152 multiplied by a calibration factor. Calibration of the instrument was carried out with diluted
153 ammonia in nitrogen and permeation tubes of methylamine, dimethylamine, trimethylamine,
154 diethylamine, and diisopropylamine (Kin-tek, USA). Due to the difficulty of obtaining a
155 calibration standard, C5 amines were assumed to have the same sensitivity as C6 amines. The
156 calibration factors for each compound and detection limits were found to be similar to the results
157 from the calibration of the instrument by [You *et al.*, 2014] (Table S1), over a period of nearly 10
158 years, demonstrating an excellent reproducibility in the instrument performance. The time
159 response of the CIMS instrument to ammonia and amines is defined as where the signal stabilizes
160 at its “double e-folded” concentration of $1/e^2$ during the calibration. Average response times for
161 ammonia and amines were smaller than 1 minute. For each 10-minute cycle of background and
162 measurement, the first two minutes of each background/measurement cycle were excluded from
163 the data analysis to allow the instrument to reach a steady concentration.

164 Meteorological data was measured concurrently on the platform by a Vaisala HMP-45c for
165 temperature and relative humidity, and a RM Young 05305 wind speed and direction sensor.
166 Additionally, CO and NO_x (NO+NO₂) were measured with Thermo 48c and Thermo 42c-TL,
167 respectively. These measurements were provided by the University of Houston.

168

169 3. Results and Discussion

170

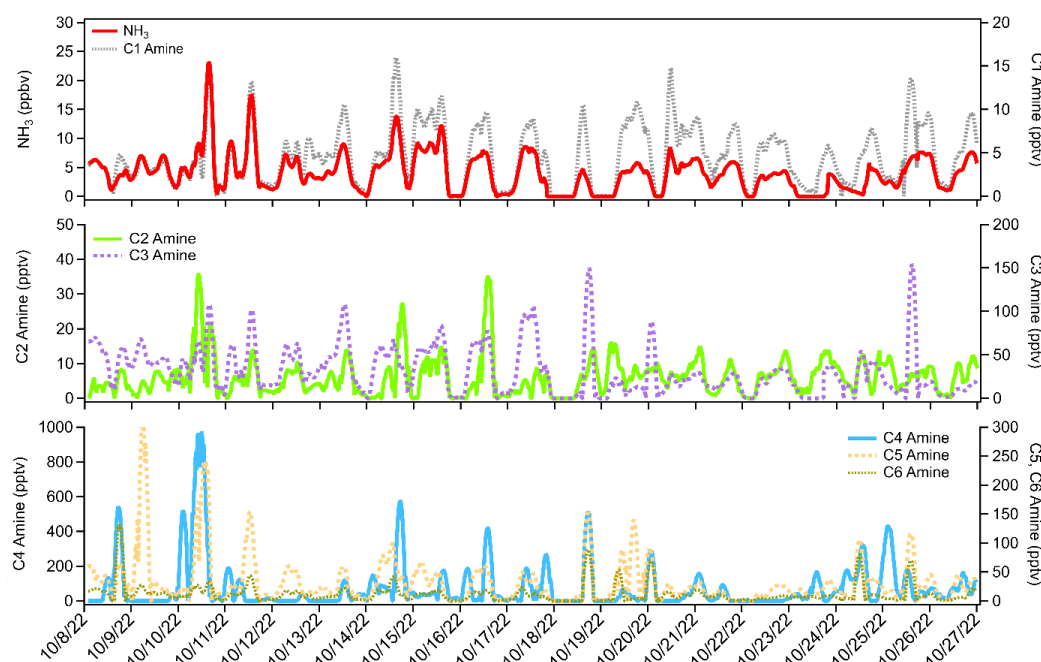
171 The time series of ammonia and amines during the ambient measurement period is shown in
172 Fig. 2. The average ammonia concentration during the measurement campaign was 4 ppbv with
173 several short-term spikes above 10 ppbv and one occasion when the concentration exceeded 20
174 ppbv. Concentrations of C1 amine averaged 4 pptv with several spikes up to 15 pptv. Average C2
175 amine concentrations were 6 pptv with frequent but brief periods of concentrations more than 10
176 pptv. Average C3 amine concentrations were 31 pptv with brief increases in concentration above
177 100 pptv. C4 amine was the most abundant amine observed during the measurement period with
178 an average concentration of 79 pptv with spikes in concentration into the hundreds of pptv.
179 Average C5 and C6 amine concentrations were 33 and 12 pptv, respectively. These concentrations
180 in Houston were generally consistent with concentrations measured in other urban sites (Table 1).
181 Ammonia concentrations of similar magnitude to the high spikes in concentration observed in this
182 study have been reported in Shanghai [S Xiao *et al.*, 2015] as well as an urban site in Romania
183 [Petruș *et al.*, 2022], with high ammonia concentrations corresponding to high temperatures and
184 high traffic activity. Long-term measurements taken in Nanjing with a cavity ring-down
185 spectrometer also showed an average ammonia concentration of 12 ppbv [Liu *et al.*, 2024].
186 Measurements of amines in Atlanta, Georgia showed <1 to 3 pptv concentrations of C1 and C2
187 amines, and C3 and C6 amines up to 15-25 pptv [Hanson *et al.*, 2011]. Yao *et al.* [Yao *et al.*, 2016]



188 measured amines at the level of pptv or sub-pptv, e.g., C2 amines of 3.9 ± 1.2 pptv, in urban
 189 Shanghai during the summer.

190

191



192

193 **Fig. 2.** Time series of ammonia and C1-C6 amines observed at the urban center in Houston, Texas,
 194 in October 2022.

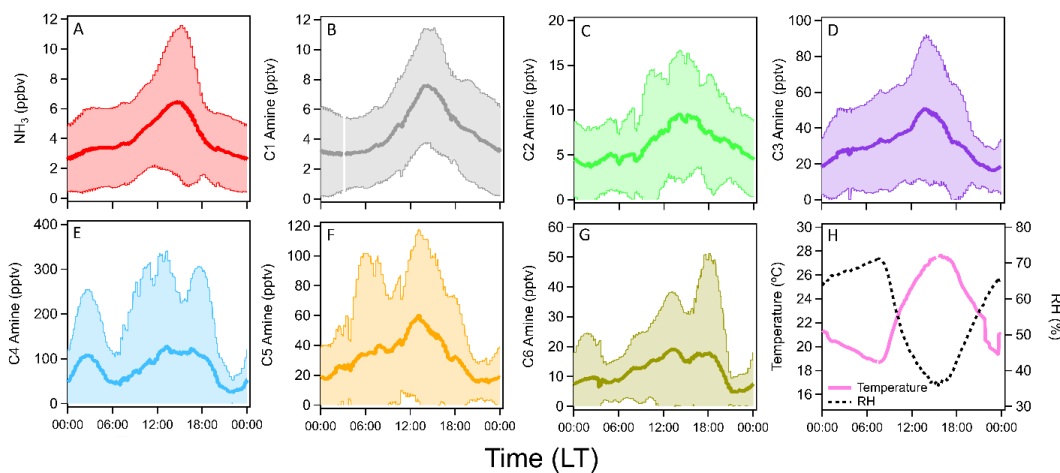
195 Figure 3 shows the averaged diurnal concentrations of ammonia and amines during the
 196 observation period. Ammonia and amines had a diurnal cycle with peak concentrations in the
 197 afternoon with higher ambient temperatures. Generally, ammonia and amines correlated with one
 198 another throughout the measurement campaign, while C1-C3 amines showed the highest
 199 correlation with ammonia. Peak concentrations of all compounds corresponded with the high
 200 temperature of the day at around 3 pm local time. This was especially pronounced for ammonia,
 201 C1 and C3 amines. The relationships between ammonia and amines and temperature are shown in
 202 Fig. 4. Ammonia had the strongest correlation with temperature, and the relationship fit an
 203 exponential parameterization, as the following:

204
$$[NH_3] = 2.85 + 9.66 \times 10^{15} e^{-\frac{10619}{T}}$$

205 Amines generally showed linear relationships with temperature, with C3 and C4 amines displaying
 206 the strongest relationships. C3 amines increased by 2.3 pptv per °C ($r^2 = 0.86$) and C4 by 2.9 pptv
 207 per °C ($r^2 = 0.65$). C5 and C6 amines were also moderately correlated with temperature, increasing
 208 by 1.2 pptv per °C and 0.5 pptv per °C, respectively ($r^2 = 0.60$ for both C5 and C6). On the other



209 hand, the correlation of C1 and C2 amines with temperature were weaker: C1 only increased by
 210 0.1 pptv per °C with almost no correlation ($r^2 = 0.22$), and C2 increased by 0.8 pptv per °C ($r^2 =$
 211 0.50). Despite this variation, elevated temperatures generally result in heightened emissions of
 212 ammonia and amines. The clear temperature dependence of ammonia and amines indicates
 213 dominant gas-to-particle conversion processes, as previously found in a rural forest in Alabama by
 214 [You *et al.*, 2014], which also showed an anticorrelation of these base compounds between gas and
 215 aerosol phases. The temperature dependence could also be due to higher emissions at higher
 216 temperatures. The temperature dependence of ammonia and amines has been observed at other
 217 locations such as Kent, Ohio [You *et al.*, 2014], Atlanta [Hanson *et al.*, 2011], Delaware [Freshour
 218 *et al.*, 2014], the Southern Great Plains [Freshour *et al.*, 2014], and a rural central Germany
 219 [Kürten *et al.*, 2016].
 220
 221



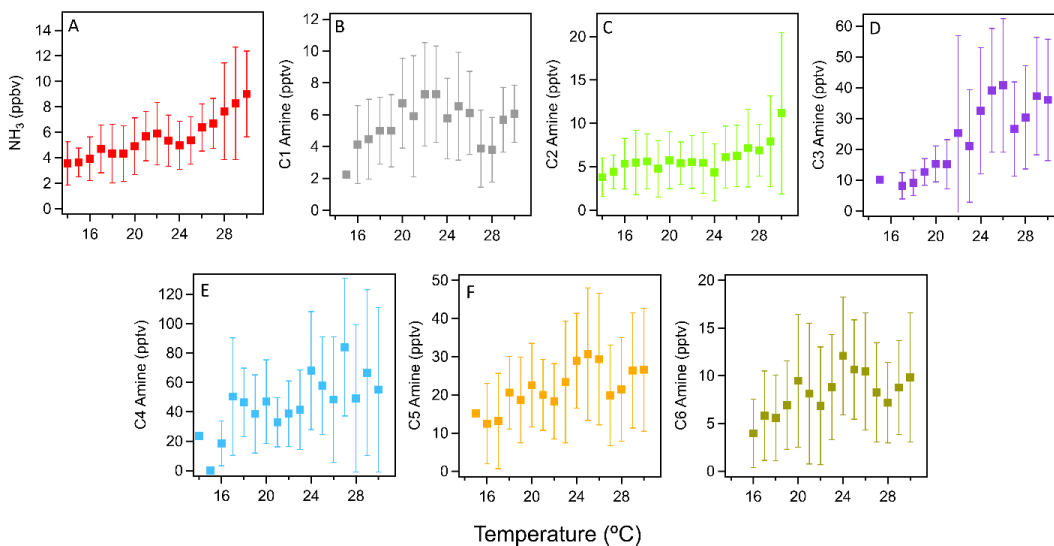
222

223 **Fig. 3.** Averaged diurnal cycles of (a) ammonia, (b-g) C1-C6 amines, (h) temperature, and RH in
 224 Houston, Texas, during the observation period (19 days continuously). Shaded areas indicate 1
 225 standard deviation from the mean values of observation data.

226

227

228



229

230

231 **Fig. 4.** Temperature dependence of (a) ammonia and (b-g) C1-C6 amines measured in Houston.
 232 Vertical bars indicate 1 standard deviation from the mean values of observation data.

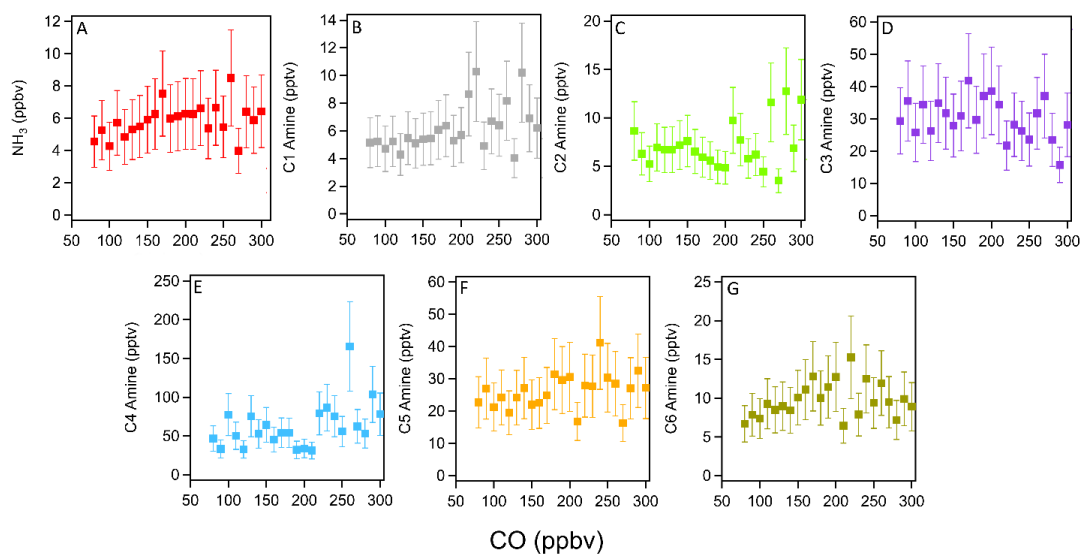
233

234 Anthropogenic pollutants such as CO and NO_x and CO can serve as tracers for industrial and
 235 traffic activities. Ammonia and amines in general showed a positive correlation with CO (Fig. 5).
 236 As ammonia, amines, and CO can be traced to traffic or industrial emissions, the positive
 237 relationship between these compounds implies that these base compounds were emitted from
 238 pollutant sources. Unlike with CO, there was a negative correlation with NO_x (Fig. S3). This lack
 239 of a strong correlation between NO_x and ammonia was previously observed in Nanjing where a
 240 strong reduction in NO_x concentration during COVID-19 lockdown periods was not accompanied
 241 by an equivalent reduction in ammonia concentrations [Liu *et al.*, 2024]. This may indicate some
 242 unique emission sources for ammonia and amines that do not co-emit NO_x.

243

244

245



246
 247 **Fig. 5.** Correlation between ammonia (a) and C1-C6 amines (b-g) with the collocated CO
 248 concentrations during the measurement campaign. Vertical bars indicate 1 standard deviation from
 249 the mean values of observation data.

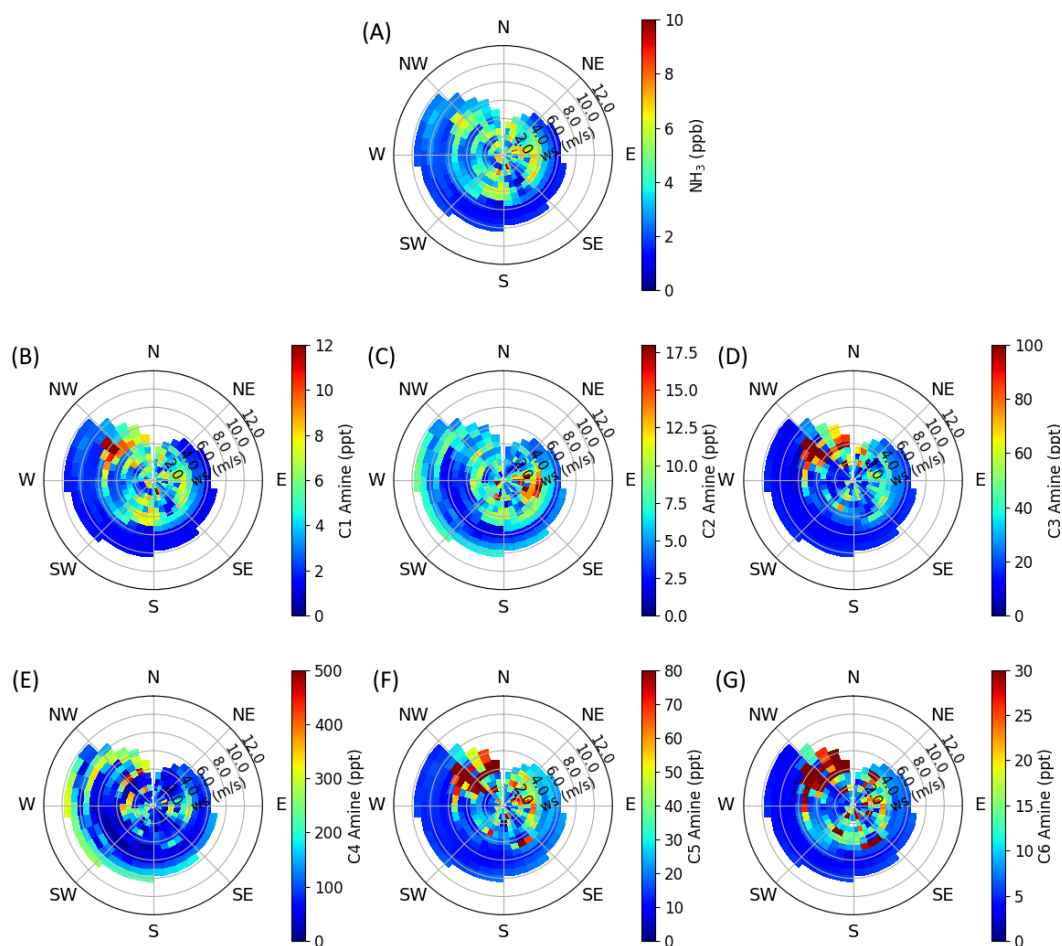
250

251 Wind speed and direction can help to identify local sources of ammonia and amines near the
 252 measurement site. Figures 6 and S4 show the correlation of ammonia and amines with wind speeds
 253 and direction throughout the observation period. Consistent between all base compounds is the
 254 high concentration coming from the southeast. This is the direction of the interstate highway,
 255 industrial areas, and train yards (Figs. 1 and S1). Ammonia and most amines also have a
 256 pronounced source from the northwest – this is the direction of downtown Houston, where
 257 population density is highest. Except for C2 and C4 amines, the observed ammonia and amines in
 258 Houston were higher during periods of low wind speeds. The abundant C2 and C4 at high wind
 259 speeds may suggest that C2 and C4 amines were transported from more distant sources.

260 Figure S5 shows the average diurnal cycle of ammonia and amines on weekdays as opposed
 261 to weekends. Except for C2 and C4 amines, there was a clear decrease in concentrations during
 262 weekends during the afternoon peak. Weekends saw much less traffic and activity on the
 263 University of Houston campus. During this observation period, ambient temperatures were higher
 264 during the weekends, which would increase emissions. Therefore, the differences in weekdays vs.
 265 weekends indicate that amines and ammonia were indeed emitted from traffic and industrial
 266 activities. Lower average amine concentrations on weekends were also observed during mobile
 267 measurements in Yangtze River Delta cities [Chang *et al.*, 2022].

268

269



270

271

272 **Fig. 6.** Wind rose plots of (a) ammonia and (b-g) C1-C6 amines observed in urban Houston. The

273 color scale indicates concentration, and radial intensity shows wind speed.

274

275

4. Atmospheric Implications

276

277

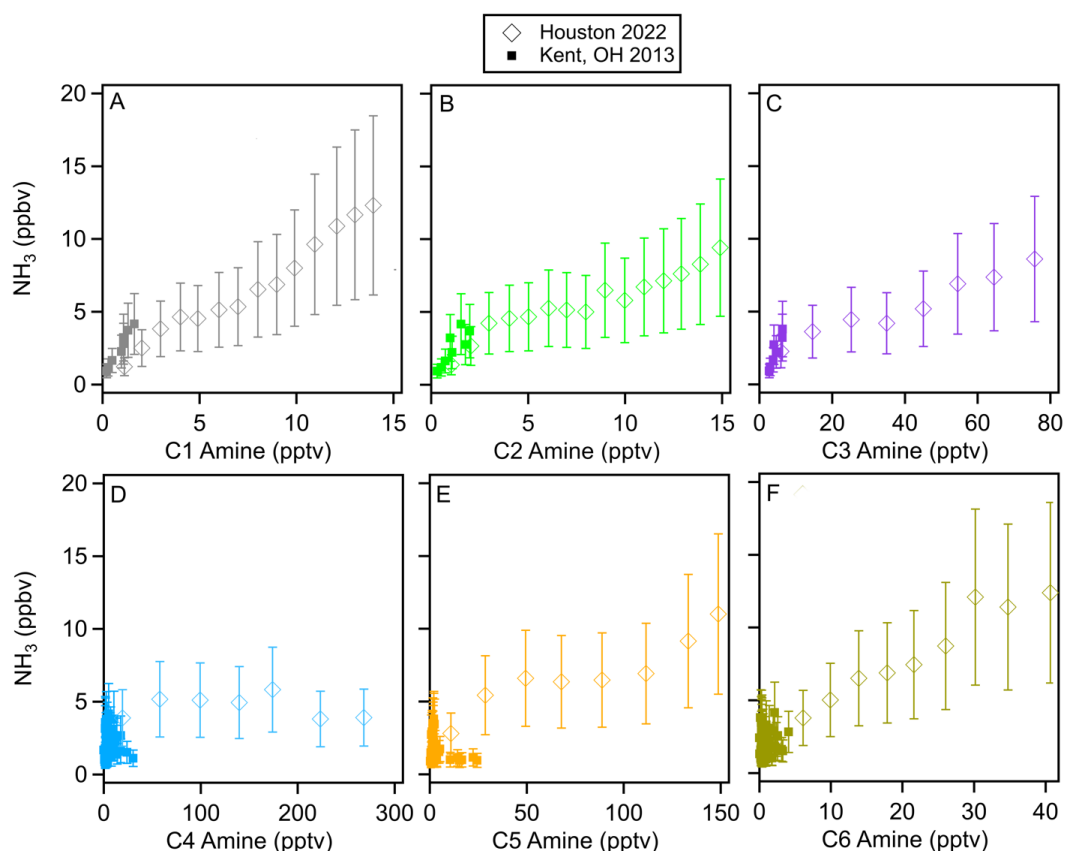
278 Field observations show that sulfuric acid and amines are responsible for aerosol nucleation
 279 [J. Brean *et al.*, 2020; R. Cai *et al.*, 2021; Runlong Cai *et al.*, 2023; Jen *et al.*, 2016; Smith *et al.*,
 280 2010; Yan *et al.*, 2021; Yao *et al.*, 2016], however, currently, global models do not have amine
 281 emission inventories. Figure 7 shows the correlation of ammonia with C1-C6 amines measured
 282 during this campaign. This figure also includes that data obtained with the same instrument in
 283 Kent, Ohio, [You *et al.*, 2014]. It is clear from this figure that concentrations of ammonia, C1, C2,
 284 C3, C5, and C6 amines were positively correlated with one another throughout the study: r^2 values
 for the correlation between ammonia and amines were 0.61 for C1, 0.42 for C2, 0.47 for C3, 0.26



285 for C5 and 0.88 for C6. These relationships imply that these compounds are mostly co-emitted
 286 from similar sources and undergo similar atmospheric transport. C4 amines showed no correlation
 287 with ammonia and lower-mass amines – the r^2 value for C4 vs. NH_3 was 0.048. This indicates a
 288 unique source for C4 amines, consistent with both elevated C4 concentrations at high wind speeds
 289 and higher weekend C4 concentrations as discussed previously. Concentrations of C1-C3 amines
 290 concentrations were approximately equivalent to $1.1 \times 10^{-3} [\text{NH}_3]$, $1.4 \times 10^{-3} [\text{NH}_3]$, and 8.4×10^{-3}
 291 $[\text{NH}_3]$, respectively. C5 and C6 amine concentrations were $1.9 \times 10^{-2} [\text{NH}_3]$ and $3.5 \times 10^{-3} [\text{NH}_3]$,
 292 respectively (Table S2). From these results, we propose that global modelers use 0.1 % of the
 293 ammonia concentration as a proxy of dimethylamine to simulate urban NPF processes.

294

295



296

297 **Fig. 7.** Correlations of C1-C6 amines with ammonia throughout the observation period in Houston
 298 (diamonds) and Kent, OH (squares) as reported by [You *et al.*, 2014]. Vertical bars indicate one
 299 standard deviation from the mean values of observation data.

300

301



302 5. Conclusions

303

304 Our observations in urban Houston show that ammonia and amines generally followed a clear
305 diurnal cycle, peaking in the early afternoon when the ambient temperature was highest during the
306 day. We found a correlation of ammonia and amines with ambient temperature. The pronounced
307 diurnal cycles and temperature dependence of these compounds may be due to active partitioning
308 between the gas and particle phases, which is sensitively dependent on temperature. This could be
309 due to increased emissions of ammonia and amines from biogenic and anthropogenic sources. It
310 is likely a combination of these effects that causes elevated ammonia and amine concentrations
311 when temperatures are high.

312 High concentrations of ammonia and amines were correlated with local air masses from
313 densely populated areas and areas of high traffic, industry, and other human activity. This suggests
314 that most ammonia and amines measured in Houston originated from pollutant sources, consistent
315 with the correlation observed with CO concentrations. There was also a clear increase in ammonia
316 and amines on days with more human activity as shown by the results of concentrations on
317 weekends vs weekdays. We observed a consistent relationship between ammonia and amines
318 during our measurement campaign as well as with observations in less densely populated Kent,
319 Ohio, suggesting that it is reasonable to parameterize amine emission inventories based on existing
320 ammonia inventories to simulate urban NPF processes.

321 The CIMS used in this campaign is currently one of the few instruments in the world that is
322 capable of simultaneous measurements of ammonia and amines at atmospherically relevant
323 detection limits and timescales. Studies have shown that the co-presence of ammonia and amines
324 can enhance sulfuric acid nucleation rates compared to ammonia alone [Glasoe *et al.*, 2015; Myllys
325 *et al.*, 2019; Yu *et al.*, 2012]. From this perspective, simultaneous measurements of ammonia and
326 amines will be required for the correct prediction of NPF processes in the atmosphere.
327 Measurements of ammonia and amines with comprehensive calibration as shown in the present
328 study are very even rarer, but such measurements are needed for mitigating urban air quality
329 problems and the health effects of ultrafine particles.

330

331 Code Availability

332 Instrumental data processing and statistical analyses were performed using Python with the
333 NumPy and Pandas libraries. Code will be available upon request (shanhu.lee@uah.edu).

334

335 Data Availability

336 Data used in this paper are available at <https://doi.org/10.5281/zenodo.11086678> [L Tiszenkel *et*
337 *al.*, 2024].

338

339 Author Contributions

340 SHL designed the research; LT and SHL performed measurements; JF provided the measurement
341 platform as well as the trace gas and meteorology data; LT and SHL wrote the manuscript.

342

343 Competing Interests

344 The authors declare no competing interests.



345

346 **Acknowledgements**

347 We acknowledge funding support from National Science Foundation (grant numbers 2209722,
348 2117389, and 2107916) and Texas Commission on Environmental Quality (grant number 582-22-
349 31535-018).



350 **Table 1.** Ammonia and amine measurements with CIMS at various locations reported in the
 351 literature. DL, detection limit of each instrument.

Location	NH ₃ (ppbv)	C1 Amine (pptv)	C2 Amine (pptv)	C3 Amine (pptv)	C4 Amine (pptv)	C5 Amine (pptv)	C6 Amine (pptv)
Rural Alabama Forest [<i>You et al.</i> , 2014]*	Up to 1-2	< DL	< DL	1 - 10	< DL	< DL	< DL
Kent, Ohio [<i>You et al.</i> , 2014]*	Up to 6	1 – 4	< DL	5 - 10	10 - 50	10 - 100	< DL
Kent, Ohio [<i>Yu and Lee</i> , 2012]*	0.5 ± 0.26	-	8 ± 3	16 ± 7	-	-	-
Atlanta, Georgia [<i>Hanson et al.</i> , 2011]†	-	< 1	3	4 – 15	25	-	-
Lewes, Delaware [<i>Freshour et al.</i> , 2014]†	0.8	5	28	6	150	1	2
Lamont, Oklahoma [<i>Freshour et al.</i> , 2014]†	0.9	4	14	35	150	98	20
Minneapolis, Minnesota [<i>Freshour et al.</i> , 2014]†	1.8	4	42	19	14	20	5
Shanghai [<i>Yao et al.</i> , 2016]‡	-	3.9 ± 1.2	6.6 ± 1.2	0.4 ± 0.1	3.6 ± 1.0	0.7 ± 0.3	1.8 ± 0.8
Nanjing [<i>Zheng et al.</i> , 2015]‡	1.7 ± 2.3	7.2 ± 7.4 (C1 + C2 + C3)			-	-	-
Wangdu	-	-	14.6 ± 14.9	-	-	-	-



[Y Wang <i>et al.</i> , 2020b]§							
Beijing [Zhu <i>et al.</i> , 2022]‡	2.8 ± 2.0	5.2 ± 4.3 (C1 + C2 + C3)	-	-	-		
Houston, TX (This study)*	4 ± 1	4 ± 2	6 ± 2	31 ± 9	79 ± 30	33 ± 12	12 ± 4

352

353 * CIMS with ethanol reagent

354 † Proton-transfer chemical ionization mass spectrometer (PTR-CIMS)

355 ‡ High-resolution time of flight chemical ionization mass spectrometer (HR-TOF CIMS) with
356 ethanol reagent

357 § Vocus proton transfer time-of-flight mass spectrometer (PTR-TOF MS)

358

359



360 References

361

362 Almeida, J., et al. (2013), Molecular understanding of sulphuric acid–amine particle nucleation
363 in the atmosphere, *Nature*, 502(7471), 359-363, doi:10.1038/nature12663.

364 Beck, L. J., et al. (2021), Differing Mechanisms of New Particle Formation at Two Arctic Sites,
365 *Geophysical Research Letters*, 48(4), e2020GL091334,
366 doi:<https://doi.org/10.1029/2020GL091334>.

367 Benson, D. R., A. Markovich, M. Al-Refai, and S. H. Lee (2010), A Chemical Ionization Mass
368 Spectrometer for ambient measurements of Ammonia, *Atmos. Meas. Tech.*, 3(4), 1075-
369 1087, doi:10.5194/amt-3-1075-2010.

370 Bianchi, F., et al. (2016), New particle formation in the free troposphere: A question of
371 chemistry and timing, *Science*, 352(6289), 1109-1112, doi:10.1126/science.aad5456.

372 Brean, J., D. C. S. Beddows, Z. Shi, B. Temime-Roussel, N. Marchand, X. Querol, A. Alastuey,
373 M. C. Minguillón, and R. M. Harrison (2020), Molecular insights into new particle
374 formation in Barcelona, Spain, *Atmos. Chem. Phys.*, 20(16), 10029-10045,
375 doi:10.5194/acp-20-10029-2020.

376 Brean, J., M. Dall'Osto, R. Simó, Z. Shi, D. C. S. Beddows, and R. M. Harrison (2021), Open
377 ocean and coastal new particle formation from sulfuric acid and amines around the
378 Antarctic Peninsula, *Nature Geoscience*, 14(6), 383-388, doi:10.1038/s41561-021-00751-
379 y.

380 Cai, R., et al. (2021), Sulfuric acid–amine nucleation in urban Beijing, *Atmos. Chem. Phys.*,
381 21(4), 2457-2468, doi:10.5194/acp-21-2457-2021.

382 Cai, R., et al. (2023), Significant contributions of trimethylamine to sulfuric acid nucleation in
383 polluted environments, *npj Climate and Atmospheric Science*, 6(1), 75,
384 doi:10.1038/s41612-023-00405-3.

385 Chang, Y., et al. (2022), Nonagricultural Emissions Dominate Urban Atmospheric Amines as
386 Revealed by Mobile Measurements, *Geophysical Research Letters*, 49(10),
387 e2021GL097640, doi:<https://doi.org/10.1029/2021GL097640>.

388 Ellis, R. A., J. G. Murphy, E. Pattey, R. van Haarlem, J. M. O'Brien, and S. C. Herndon (2010),
389 Characterizing a Quantum Cascade Tunable Infrared Laser Differential Absorption
390 Spectrometer (QC-TILDAS) for measurements of atmospheric ammonia, *Atmos. Meas.*
391 *Tech.*, 3(2), 397-406, doi:10.5194/amt-3-397-2010.

392 Erupe, M. E., et al. (2010), Correlation of aerosol nucleation rate with sulfuric acid and ammonia
393 in Kent, Ohio: An atmospheric observation, *Journal of Geophysical Research:*
394 *Atmospheres*, 115(D23), doi:<https://doi.org/10.1029/2010JD013942>.

395 Erupe, M. E., A. A. Viggiano, and S. H. Lee (2011), The effect of trimethylamine on
396 atmospheric nucleation involving H₂SO₄, *Atmos. Chem. Phys.*, 11, 4767-4775.

397 Freshour, N. A., K. K. Carlson, Y. A. Melka, S. Hinz, B. Panta, and D. R. Hanson (2014), Amine
398 permeation sources characterized with acid neutralization and sensitivities of an amine
399 mass spectrometer, *Atmos. Meas. Tech.*, 7(10), 3611-3621, doi:10.5194/amt-7-3611-
400 2014.

401 Ge, X., A. S. Wexler, and S. L. Clegg (2011a), Atmospheric amines – Part I. A review,
402 *Atmospheric Environment*, 45(3), 524-546,
403 doi:<https://doi.org/10.1016/j.atmosenv.2010.10.012>.



- 404 Ge, X., A. S. Wexler, and S. L. Clegg (2011b), Atmospheric amines – Part II. Thermodynamic
405 properties and gas/particle partitioning, *Atmospheric Environment*, 45(3), 561-577,
406 doi:<https://doi.org/10.1016/j.atmosenv.2010.10.013>.
- 407 Glasoe, W. A., K. Volz, B. Panta, N. Freshour, R. Bachman, D. R. Hanson, P. H. McMurry, and
408 C. Jen (2015), Sulfuric acid nucleation: an experimental study of the effect of seven
409 bases, *J. Geophys. Res.*, 120, 1933-1950, doi:Doi: 10.1002/2014JD022730.
- 410 Griffith, D. W. T., and B. Galle (2000), Flux measurements of NH₃, N₂O and CO₂ using dual
411 beam FTIR spectroscopy and the flux–gradient technique, *Atmospheric Environment*,
412 34(7), 1087-1098, doi:[https://doi.org/10.1016/S1352-2310\(99\)00368-4](https://doi.org/10.1016/S1352-2310(99)00368-4).
- 413 Gu, B., et al. (2021), Abating ammonia is more cost-effective than nitrogen oxides for mitigating
414 PM_{2.5} air pollution, *Science*, 374(6568), 758-762, doi:10.1126/science.abf8623.
- 415 Hanson, D. R., P. H. McMurry, J. Jiang, D. Tanner, and L. G. Huey (2011), Ambient Pressure
416 Proton Transfer Mass Spectrometry: Detection of Amines and Ammonia, *Environmental
417 Science & Technology*, 45(20), 8881-8888, doi:10.1021/es201819a.
- 418 Jen, C. N., R. Bachman, J. Zhao, P. H. McMurry, and D. R. Hanson (2016), Diamine-sulfuric
419 acid reactions are a potent source of new particle formation, *Geophysical Research
420 Letters*, 43(2), 867-873, doi:<https://doi.org/10.1002/2015GL066958>.
- 421 Jokinen, T., et al. Ion-induced sulfuric acid–ammonia nucleation drives particle formation in
422 coastal Antarctica, *Science Advances*, 4(11), eaat9744, doi:10.1126/sciadv.aat9744.
- 423 Köllner, F., et al. (2017), Particulate trimethylamine in the summertime Canadian high Arctic
424 lower troposphere, *Atmos. Chem. Phys.*, 17(22), 13747-13766, doi:10.5194/acp-17-
425 13747-2017.
- 426 Kürten, A., A. Bergen, M. Heinritzi, M. Leiminger, V. Lorenz, F. Piel, M. Simon, R. Sitals, A.
427 C. Wagner, and J. Curtius (2016), Observation of new particle formation and
428 measurement of sulfuric acid, ammonia, amines and highly oxidized organic molecules at
429 a rural site in central Germany, *Atmos. Chem. Phys.*, 16(19), 12793-12813,
430 doi:10.5194/acp-16-12793-2016.
- 431 Lee, S.-H. (2022), Perspective on the Recent Measurements of Reduced Nitrogen Compounds in
432 the Atmosphere, *Frontiers in Environmental Science*, 10,
433 doi:10.3389/fenvs.2022.868534.
- 434 Leen, J. B., X.-Y. Yu, M. Gupta, D. S. Baer, J. M. Hubbe, C. D. Kluzek, J. M. Tomlinson, and
435 M. R. Hubbell, II (2013), Fast In Situ Airborne Measurement of Ammonia Using a Mid-
436 Infrared Off-Axis ICOS Spectrometer, *Environmental Science & Technology*, 47(18),
437 10446-10453, doi:10.1021/es401134u.
- 438 Lehtipalo, K., et al. (2018), Multicomponent new particle formation from sulfuric acid,
439 ammonia, and biogenic vapors, *Science Advances*, 4(12), eaau5363,
440 doi:10.1126/sciadv.aau5363.
- 441 Liu, R., et al. (2024), Characteristics and sources of atmospheric ammonia at the SORPES
442 station in the western Yangtze river delta of China, *Atmospheric Environment*, 318,
443 120234, doi:<https://doi.org/10.1016/j.atmosenv.2023.120234>.
- 444 Malloy, Q. G. J., Q. Li, B. Warren, D. R. Cocker III, M. E. Erupe, and P. J. Silva (2009),
445 Secondary organic aerosol formation from primary aliphatic amines with
446 NO₃ radical, *Atmos. Chem. Phys.*, 9(6), 2051-2060, doi:10.5194/acp-9-
447 2051-2009.



- 448 Martin, N. A., V. Ferracci, N. Cassidy, and J. A. Hoffnagle (2016), The application of a cavity
449 ring-down spectrometer to measurements of ambient ammonia using traceable primary
450 standard gas mixtures, *Applied Physics B*, 122(8), 219, doi:10.1007/s00340-016-6486-9.
- 451 McManus, J. B., S. Z. Mark, D. N. David, Jr., H. S. Joanne, C. H. Scott, C. W. Ezra, and W.
452 Rick (2010), Application of quantum cascade lasers to high-precision atmospheric trace
453 gas measurements, *Optical Engineering*, 49(11), 111124, doi:10.1117/1.3498782.
- 454 Miller, D. J., K. Sun, L. Tao, M. A. Khan, and M. A. Zondlo (2014), Open-path, quantum
455 cascade-laser-based sensor for high-resolution atmospheric ammonia measurements,
456 *Atmos. Meas. Tech.*, 7(1), 81-93, doi:10.5194/amt-7-81-2014.
- 457 Myllys, N., S. Chee, T. Olenius, M. Lawler, and J. Smith (2019), Molecular-Level
458 Understanding of Synergistic Effects in Sulfuric Acid–Amine–Ammonia Mixed Clusters,
459 *The Journal of Physical Chemistry A*, 123(12), 2420-2425,
460 doi:10.1021/acs.jpca.9b00909.
- 461 Nielsen, C. J. (2016), Atmospheric Degradation of Amines (ADA). Summary report: Photo-
462 oxidation of methylamine, dimethylamine and trimethylamine. CLIMIT project no.
463 201604., *Norge: Norsk Institutt for Luftforskning*.
- 464 Nielsen, C. J., H. Herrmann, and C. Weller (2012), Atmospheric chemistry and environmental
465 impact of the use of amines in carbon capture and storage (CCS), *Chemical Society*
466 *Reviews*, 41(19), 6684-6704, doi:10.1039/C2CS35059A.
- 467 Nowak, J. B., et al. (2006), Analysis of urban gas phase ammonia measurements from the 2002
468 Atlanta Aerosol Nucleation and Real-Time Characterization Experiment (ANARChE),
469 *Journal of Geophysical Research: Atmospheres*, 111(D17),
470 doi:<https://doi.org/10.1029/2006JD007113>.
- 471 Petrus, M., C. Popa, and A. M. Bratu (2022), Ammonia Concentration in Ambient Air in a Peri-
472 Urban Area Using a Laser Photoacoustic Spectroscopy Detector, *Materials (Basel)*,
473 15(9), doi:10.3390/ma15093182.
- 474 Pollack, I. B., J. Lindaas, J. R. Roscioli, M. Agnese, W. Permar, L. Hu, and E. V. Fischer (2019),
475 Evaluation of ambient ammonia measurements from a research aircraft using a closed-
476 path QC-TILDAS operated with active continuous passivation, *Atmos. Meas. Tech.*,
477 12(7), 3717-3742, doi:10.5194/amt-12-3717-2019.
- 478 Pushkarsky, M. B., M. E. Webber, O. Baghdassarian, L. R. Narasimhan, and C. K. N. Patel
479 (2002), Laser-based photoacoustic ammonia sensors for industrial applications, *Applied*
480 *Physics B*, 75(2), 391-396, doi:10.1007/s00340-002-0967-8.
- 481 Qiu, C., and R. Zhang (2013), Multiphase chemistry of atmospheric amines, *Physical Chemistry*
482 *Chemical Physics*, 15(16), 5738-5752, doi:10.1039/C3CP43446J.
- 483 Schwab, J. J., Y. Li, M. S. Bae, K. L. Demerjian, J. Hou, X. Zhou, B. Jensen, and S. C. Pryor
484 (2007), A laboratory intercomparison of real-time gaseous ammonia measurement
485 methods, *Environ Sci Technol*, 41(24), 8412-8419, doi:10.1021/es070354r.
- 486 Silva, P. J., M. E. Erupe, D. Price, J. Elias, Q. G. J. Malloy, Q. Li, B. Warren, and D. R. Cocker,
487 III (2008), Trimethylamine as Precursor to Secondary Organic Aerosol Formation via
488 Nitrate Radical Reaction in the Atmosphere, *Environmental Science & Technology*,
489 42(13), 4689-4696, doi:10.1021/es703016v.
- 490 Smith, J. N., K. C. Barsanti, H. R. Friedli, M. Ehn, M. Kulmala, D. R. Collins, J. H. Scheckman,
491 B. J. Williams, and P. H. McMurry (2010), Observations of aminium salts in atmospheric
492 nanoparticles and possible climatic implications, *Proc. Natl. Acad. Sci.*, 107(15), 6634-
493 6639.



- 494 Tiszenkel, L., J. Flynn, and S.-H. Lee (2024), Data Used in Manuscript Entitled "Measurement
495 Report: Urban Ammonia and Amines in Houston, Texas", edited, Zenodo,
496 doi:<https://doi.org/10.5281/zenodo.11086678>.
- 497 Tiszenkel, L., and S.-H. Lee (2023), Synergetic Effects of Isoprene and HO_x on Biogenic New
498 Particle Formation, *Geophysical Research Letters*, 50(14), e2023GL103545,
499 doi:<https://doi.org/10.1029/2023GL103545>.
- 500 Tiszenkel, L., C. Stangl, J. Krasnomowitz, Q. Ouyang, H. Yu, M. J. Apsokardu, M. V. Johnston,
501 and S. H. Lee (2019), Temperature effects on sulfuric acid aerosol nucleation and growth:
502 initial results from the TANGENT study, *Atmos. Chem. Phys.*, 19(13), 8915-8929,
503 doi:10.5194/acp-19-8915-2019.
- 504 Wang, G., et al. (2016), Persistent sulfate formation from London Fog to Chinese haze,
505 *Proceedings of the National Academy of Sciences*, 113(48), 13630-13635,
506 doi:10.1073/pnas.1616540113.
- 507 Wang, M., et al. (2020a), Rapid growth of new atmospheric particles by nitric acid and ammonia
508 condensation, *Nature*, 581(7807), 184-189, doi:10.1038/s41586-020-2270-4.
- 509 Wang, Y., G. Yang, Y. Lu, Y. Liu, J. Chen, and L. Wang (2020b), Detection of gaseous
510 dimethylamine using vocus proton-transfer-reaction time-of-flight mass spectrometry,
511 *Atmospheric Environment*, 243, 117875,
512 doi:<https://doi.org/10.1016/j.atmosenv.2020.117875>.
- 513 Xiao, M., et al. (2021), The driving factors of new particle formation and growth in the polluted
514 boundary layer, *Atmos. Chem. Phys.*, 21(18), 14275-14291, doi:10.5194/acp-21-14275-
515 2021.
- 516 Xiao, S., et al. (2015), Strong atmospheric new particle formation in winter in urban Shanghai,
517 China, *Atmos. Chem. Phys.*, 15(4), 1769-1781, doi:10.5194/acp-15-1769-2015.
- 518 Yan, C., et al. (2021), The Synergistic Role of Sulfuric Acid, Bases, and Oxidized Organics
519 Governing New-Particle Formation in Beijing, *Geophysical Research Letters*, 48(7),
520 e2020GL091944, doi:<https://doi.org/10.1029/2020GL091944>.
- 521 Yao, L., et al. (2016), Detection of atmospheric gaseous amines and amides by a high-resolution
522 time-of-flight chemical ionization mass spectrometer with protonated ethanol reagent
523 ions, *Atmos. Chem. Phys.*, 16(22), 14527-14543, doi:10.5194/acp-16-14527-2016.
- 524 You, Y., et al. (2014), Atmospheric amines and ammonia measured with a Chemical Ionization
525 Mass Spectrometer (CIMS), *Atmos. Chem. Phys.*, 14, 12181-12194, doi:Doi:
526 10.5194/acpd-14-16411-2014.
- 527 Yu, H., and S. H. Lee (2012), A chemical ionization mass spectrometer for the detection of
528 atmospheric amines, *Environ. Chem.*, 9, 190-201.
- 529 Yu, H., R. McGraw, and S. H. Lee (2012), Effects of amines on formation of sub-3 nm particles
530 and their subsequent growth, *Geophys. Res. Lett.*, 39, Doi: 10.1029/2011gl050099,
531 doi:10.1029/2011gl050099.
- 532 Zheng, J., Y. Ma, M. Chen, Q. Zhang, L. Wang, A. F. Khalizov, L. Yao, Z. Wang, X. Wang, and
533 L. Chen (2015), Measurement of atmospheric amines and ammonia using the high
534 resolution time-of-flight chemical ionization mass spectrometry, *Atmospheric
535 Environment*, 102, 249-259, doi:<https://doi.org/10.1016/j.atmosenv.2014.12.002>.
- 536 Zhu, S., et al. (2022), Observation and Source Apportionment of Atmospheric Alkaline Gases in
537 Urban Beijing, *Environmental Science & Technology*, 56(24), 17545-17555,
538 doi:10.1021/acs.est.2c03584.
- 539